

Observation of sheath structure near a rf electrode in a magnetized afterglow plasma

Yoshihiro Okuno, Shinya Yagura, and Hiroharu Fujita

Citation: [Journal of Applied Physics](#) **65**, 2205 (1989); doi: 10.1063/1.342831

View online: <http://dx.doi.org/10.1063/1.342831>

View Table of Contents: <http://scitation.aip.org/content/aip/journal/jap/65/6?ver=pdfcov>

Published by the [AIP Publishing](#)

Articles you may be interested in

[Sheath structure in a magnetized plasma](#)

Phys. Fluids B **5**, 1723 (1993); 10.1063/1.860806

[Particle simulation of the magnetized rf plasma sheath](#)

Phys. Fluids B **4**, 2699 (1992); 10.1063/1.860139

[Collisionless Sheath near an Electrode in the Presence of a Magnetic Field](#)

Phys. Fluids **14**, 344 (1971); 10.1063/1.1693434

[Surface Effects on the Structure of a Collisionless Sheath near an Electrode](#)

Phys. Fluids **11**, 1085 (1968); 10.1063/1.1692047

[Collisionless Theory of a Plasma Sheath near an Electrode](#)

Phys. Fluids **9**, 2168 (1966); 10.1063/1.1761586



Powerful, Multi-functional UV-Vis-NIR and FTIR Spectrophotometers

Providing the utmost in sensitivity, accuracy and resolution for applications in materials characterization and nano research

- Photovoltaics
- Polymers
- Thin films
- Paints
- Ceramics
- DNA film structures
- Coatings
- Packaging materials

[Click here to learn more](#)



Observation of sheath structure near a rf electrode in a magnetized afterglow plasma

Yoshihiro Okuno,^{a)} Shinya Yagura,^{a)} and Hiroharu Fujita^{a)}
Institute of Plasma Physics, Nagoya University, Nagoya 464, Japan

(Received 22 September 1988; accepted for publication 14 November 1988)

The sheath structure near a rf electrode has been observed by measuring the spatial profiles of the potential and density in a magnetized afterglow plasma. Dependence of the structure on the rf frequency (10–40 MHz) and elapsed time during the afterglow in a periodic, pulsed rf discharge operation are obtained by a time resolved measuring method. The potential close to the electrode is found to increase with increasing frequency and with elapsed afterglow time, without much change of the density profile. In addition, a slight decrease of the electron temperature has been observed during the afterglow time, although the density is roughly constant.

I. INTRODUCTION

Radio frequency (rf) power, the frequency of which is 13.56 MHz in most cases, has been extensively used for low-pressure plasma production in plasma processing.¹ The power is normally transmitted into a vacuum tank through a capacitor² or an inductor.³ In capacitive coupling, an ambipolar dc potential appears on a rf electrode immersed in a plasma discharge, producing a sheath. The sheath structure near the rf electrode has not been studied in detail. This may be the case because of the difficulty of the probe measurement technique for such plasma parameters as the plasma potential and the density and temperature of electrons, in the presence of large-amplitude rf power.⁴ Recent plasma processing techniques have widely used the rf plasma sources, and thin-film preparation has been carried out, without knowledge of the detailed mechanism of rf plasma discharges, especially the sheath structure near rf electrodes. The characteristics of this sheath might strongly affect the thin-film quality.

In order to understand the sheath structure, valid measurements of the electric field or the potential in the sheath are required. Recently, a laser-aided field measurement⁵ has been used, but it has not yet been satisfactorily demonstrated. Besides this technique, Langmuir probe methods might become useful, even in the rf plasma, if the plasma parameters are measured just after turning off the rf power. Then, the floating potential V_f (at which the probe net current becomes zero) might be used to estimate the plasma potential. This is because the potential V_f of an emissive probe⁶ is very close to the space potential V_0 . In this conventional method, however, a poor time resolution of the measurement is usual because of a long time constant resulting from the high impedance required to make a valid measurement of V_f . To deal with this problem, we have developed an improved technique to obtain a high time resolution ($\approx 1 \mu\text{s}$) for the potential measurement with an emissive probe.⁷

In this paper, we present experimental measurements of the sheath structure by measuring the spatial profiles of the

floating potential and ion density near the rf electrode in the afterglow plasma (100–250 μs). In addition, time variations of electron density and temperature during the afterglow are discussed.

II. EXPERIMENTAL PROCEDURE

The experiments were performed in a stainless-steel vacuum tank (TPS machine; Test Plasma Small) at the Institute of Plasma Physics, Nagoya University. The diameter and length of the tank were 35 and 160 cm, respectively. An axial magnetic field of 60 G was applied to suppress plasma loss to the tank wall. A rf plane electrode 20 cm in diameter was immersed with its surface perpendicular to the plasma axis, as shown in Fig. 1. rf power was supplied from a signal generator (S.G.) through a linear amplifier in the frequency range 10–40 MHz. This system can modulate the rf signal to obtain pulsed rf power with a very quick rise and fall time ($< 50 \text{ ns}$). Here, the rf power was transmitted through a capacitor. A 50- Ω dummy load was connected to the terminal of the rf transmission line for matching.

Argon gas was introduced into the tank with a pressure of 3×10^{-4} Torr. The local potential was measured with an emissive probe (e.p.)⁶ by the improved⁷ technique to mea-

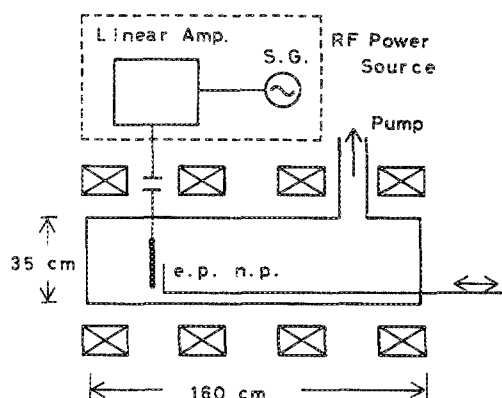


FIG. 1. Experimental apparatus. e.p. and n.p. are emissive probe and needle probe, respectively. S.G. is signal generator.

^{a)} Present address: Department of Electrical Engineering, Saga University, Honjo-machi 1, Saga 840, Japan.

sure a quickly changing potential with a high time resolution. A cylindrical needle probe (n.p.; 1 mm in diameter and 5 mm in length) highly negatively biased (-90 V) was used to collect ion saturation current. It was assumed that the current was proportional to the ion density.⁴ Furthermore, the electron temperature and density during the afterglow time were estimated from the V - I characteristics of the needle probe. The emissive and needle probes mounted on the same shaft were moved axially to measure the potential and ion density profiles near the rf electrode.

III. EXPERIMENTAL RESULTS AND DISCUSSION

Figure 2 shows the time variation of ion saturation current, I_i , collected by a negatively biased needle probe at $z = 10$ cm from the rf electrode surface (upper trace), and the rf signal (lower trace). The rf power is periodically supplied for 2.4 ms and cut off for $100\ \mu\text{s}$ with a rise and fall time below 50 ns. The off time of the rf power is short enough to regard the modulated rf power as continuous. As seen in this figure, the rf noise, when plasma production is stopped by switching off the rf power, disappears from I_i , that is, the plasma becomes quiescent. This result implies that measurement by such a probe may lead to an erroneous estimate of the plasma parameters during rf plasma production. The parameters should be measured in the absence of the rf power. It is also seen in this figure that I_i , which corresponds to the ion density, decays by about one-third during $100\ \mu\text{s}$. The overshoot of I_i after switching on the rf power in the upper trace might be caused by a transient of the rf power. This could result, not from the increase in plasma density, but from the instantaneous potential rise due to this transient. Thus, the potential shift would cause the apparent increase in I_i for the fixed biased probe.

Spatial profiles of the ion density (I_i) and the potential

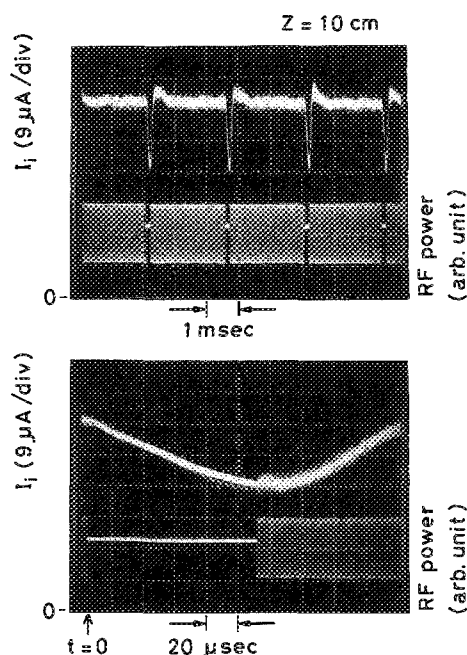


FIG. 2. Time variation of ion saturation current I_i collected by a needle probe located at $z = 10$ cm and supplied rf power. $t = 0$ corresponds to a time when the rf power is cut off.

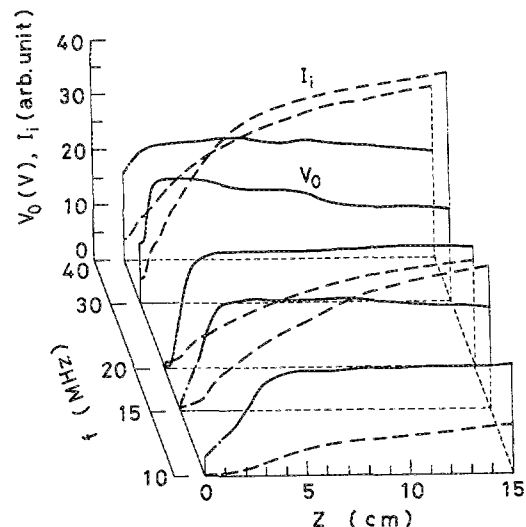


FIG. 3. Spatial profiles of the ion saturation current I_i and the potential V_0 at various rf frequencies. The data are obtained at $t = 1\ \mu\text{s}$, and $z = 0$ corresponds to the rf electrode surface.

(V_0) are measured from a point close to the electrode surface along the axial direction for various rf frequencies, as shown in Fig. 3. These profiles are obtained $1\ \mu\text{s}$ after cutting off the rf power by a sampling technique based on a repetitive supply of the rf power. Since the time resolution of the potential measurement is about $1\ \mu\text{s}$ and the rf frequency is higher than 10 MHz, the potential in Fig. 3 indicates the averaged value, even if the rf oscillation would influence the potential during the afterglow. It is seen in this figure that the potential profile forms an ion sheath structure at each frequency. Moreover, the sheath thickness estimated by the potential profile (the distance from the electrode surface to arrive at the plasma potential) decreases with increasing rf frequency.

The physical reason for ion sheath formation is as follows. The absorption of electrons from the plasma into the rf electrode is much greater than that of ions because of its oscillating potential with a frequency higher than ion plasma frequency (≈ 660 kHz) and lower than the electron plasma frequency (≈ 180 MHz). The electrode becomes self-biased negatively with respect to the plasma potential to suppress the excessive absorption of electrons in steady state. This results in ion sheath formation. The dependence of the sheath thickness on the rf frequency is considered as follows. The potential at the closest point to the electrode corresponding to a self-biased potential increases with the frequency, while the potential far from the electrode, or the plasma potential, are roughly constant. The potential rise with the frequency indicates that the number of absorbed electrons decreases with the frequency, that is, electrons become hard to follow in the rf electric field at higher frequency. Thus, the potential difference between the electrode and the plasma decreases with the frequency. The density profiles, on the other hand, are almost unchanged for various frequencies, although the density slightly increases with the frequency. Here, the rf output power from the linear amplifier was kept constant. The transmission efficiency, however,

might change owing to the simple rf matching system (50- Ω dummy load), leading to change of the power actually transmitted into the plasma. Since the ion density is not likely to depend on the frequency, the slight increase in density would be caused by a slight increase in effective power with the frequency. This power, unfortunately, was not measured.

From the above discussion, the decrease in sheath thickness should be due not to the increase in the plasma density but to the decrease in the potential difference between the electrode and the plasma. The sheath thickness is proportional to the electrode potential depth and the Debye length, which is inversely proportional to the square root of the plasma density. Thus, the electrode potential depth is more effective for the thickness than the plasma density. The decrease in the sheath thickness was confirmed from direct observation of brightness around the electrode.

Temporal evolution of the potential and density profiles were measured after cutting off the rf power, as shown in Fig. 4. It is seen that the potential close to the electrode ($z \approx 0$ cm) shifts in time toward a positive potential. It is considered that the absorption of electrons has stopped by cutting off the rf power. Then, the electrode, negatively self-biased with respect to the plasma potential, begins to absorb only ions, resulting in the potential rise of the electrode. The plasma potential in the region far from the electrode remains roughly constant, as seen in this figure. This is because the number of absorbed ions is negligible compared to that in the plasma, and no drastic change of plasma parameters such as electron density and temperature is observed, as will be described below. The density profile does not change so re-

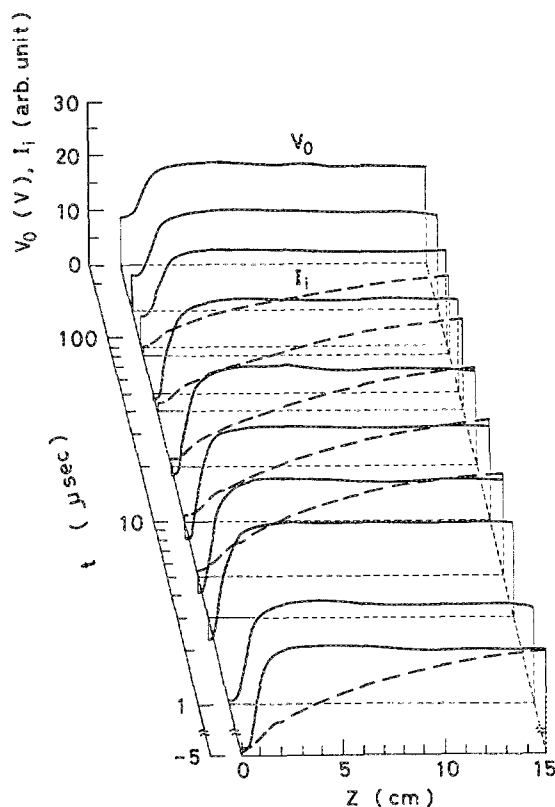


FIG. 4. Temporal evolution of spatial profiles of I_i and V_0 during the afterglow time at $f = 20$ MHz.

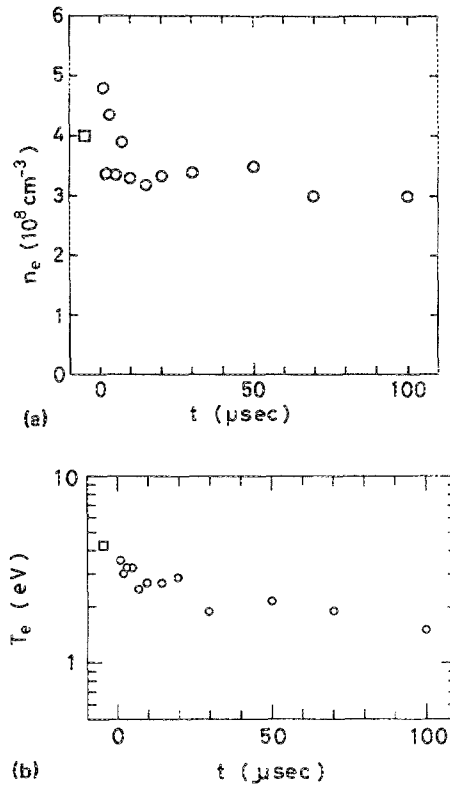


FIG. 5. Time variation of (a) electron density n_e and (b) electron temperature T_e during the afterglow time at $f = 20$ MHz, $z = 10$ cm.

markably, but the density gradient becomes slightly lower. This unresponsiveness of the density profile to variation of the sheath potential is consistent with the result in Fig. 3. Thus, sheath structure should be studied from a direct measurement of potential profile rather than the density profile. In fact, the sheath structure has been discussed from the potential profile.⁸

In addition to the above observation, time variations of the electron density n_e and electron temperature T_e during afterglow time are observed, as shown in Figs. 5(a) and 5(b), respectively. The density in Fig. 5(a) is estimated from an electron saturation current in the probe characteristic. The density remains roughly constant because of a short afterglow time, although it oscillates just after cutting off the rf power. This might be due to a transient caused by switching off the rf voltage. The ion saturation current collected by the negatively biased probe, on the contrary, decayed by about one-third, as shown in Fig. 2. We believe that there is no essential discrepancy between the results of Figs. 2 and 5(a), taking into account the decay of electron temperature, the time variation of which will be discussed later. Here, the ion saturation current I_i is proportional to the density and the square root of the electron temperature. In Fig. 5(a) the density measured during the afterglow seems to be effectively the same as the density under the rf power supply, marked by a square ($t < 0$). This result can be attributed to the small rf power supplied for plasma production. It is probably not applicable for large rf power levels, although the details have not been investigated. On the other hand, the electron temperature T_e in Fig. 5(b) decays slightly, in contrast to the

electron density, except for the duration just after the rf power is turned off. This decay can be explained by taking into account electron energy losses due to excitation, ionization, and line radiation, as well as conventional elastic collisions. Details will be reported in another paper.

IV. CONCLUSIONS

The sheath structure near a rf electrode has been studied experimentally by measuring the spatial profiles of the potential and density in afterglow of a magnetized, cylindrical argon plasma. As the rf frequency is increased, the potential close to the electrode rises, with the plasma potential remaining constant. Measurement of the temporal evolution of the profiles reveals a potential rise near the electrode. These results can be explained by considering absorption of electrons and ions on the electrode. In contrast to the behavior of the potential, no remarkable change of the density profile is observed. In addition, time variations of the density and temperature of electrons during the afterglow have been measured. The density remains roughly constant, while the electron temperature decays slightly. The plasma parameters can be measured by a probe during a short afterglow time. The experimental results above may be useful to help

understand rf plasma production techniques used in plasma processing.

ACKNOWLEDGMENTS

The authors would like to thank Dr. T. Shoji for his kind attention to this work. They also express their appreciation to the Institute of Plasma Physics, Nagoya University, where this experiment was performed under a collaborating research program. They are also grateful to the Grant-in-Aid for Scientific Research from the Japanese Ministry of Education, Science and Culture.

¹M. J. Kushner, IEEE Trans. Plasma Sci. **PS-14**, 77 (1986).

²J. L. Vossen, J. Electrochem. Soc. **126**, 319 (1979).

³T. B. Reed, J. Appl. Phys. **32**, 821 (1961).

⁴F. F. Chen, *Plasma Diagnostic Techniques*, edited by R. H. Huddleston and S. L. Leonard (Academic, New York, 1965), p. 113.

⁵B. N. Ganguly, J. R. Shoemaker, B. L. Preppernau, and A. Garscadden, J. Appl. Phys. **61**, 2778 (1987).

⁶I. Langmuir and K. T. Compton, Rev. Mod. Phys. **3**, 191 (1931).

⁷H. Fujita and S. Yagura, Jpn. J. Appl. Phys. **22**, 148 (1983).

⁸D. Bohm, *The Characteristics of Electrical Discharges in Magnetic Fields* (McGraw-Hill, New York, 1949).